ACS Catalysis

Research Article

Cite This: ACS Catal. 2017, 7, 7558-7566

pubs.acs.org/acscatalysis

Light-Driven H_2 Evolution and C=C or C=O Bond Hydrogenation by *Shewanella oneidensis*: A Versatile Strategy for Photocatalysis by Nonphotosynthetic Microorganisms

Sam F. Rowe,[†] Gwénaëlle Le Gall,[‡] Emma V. Ainsworth,[†] Jonathan A. Davies,[§] Colin W. J. Lockwood,[†] Liang Shi,[∥] Adam Elliston,[‡] Ian N. Roberts,[‡] Keith W. Waldron,[‡] David J. Richardson,[§] Thomas A. Clarke,[§] Lars J. C. Jeuken,*[,⊥] Erwin Reisner,*[,▽] and Julea N. Butt*[,†,§]

[†]School of Chemistry, University of East Anglia, Norwich Research Park, Norwich NR4 7TJ, U.K.

[‡]Quadram Institute for Bioscience, Norwich Research Park, Norwich NR4 7UA, U.K.

[§]School of Biological Sciences, University of East Anglia, Norwich Research Park, Norwich NR4 7TJ, U.K.

[∥]Department of Biological Sciences and Technology, China University of Geoscience in Wuhan, Wuhan 430074, People's Republic of China

[⊥]School of Biomedical Sciences, University of Leeds, Leeds LS2 9JT, U.K.

[▽]Department of Chemistry, University of Cambridge, Lensfield Road, Cambridge CB2 1EW, U.K.

Supporting Information

ABSTRACT: Photocatalytic chemical synthesis by coupling abiotic photosensitizers to purified enzymes provides an effective way to overcome the low conversion efficiencies of natural photosynthesis while exploiting the high catalytic rates and selectivity of enzymes as renewable, earth-abundant electrocatalysts. However, the selective synthesis of multiple products requires more versatile approaches and should avoid the time-consuming and costly processes of enzyme purification. Here we demonstrate a cell-based strategy supporting light-driven H_2 evolution or the hydrogenation of C=C and C=O bonds in a nonphotosynthetic microorganism. Methylviologen shuttles photoenergized electrons from water-soluble photosensitizers to enzymes that catalyze H_2 evolution and the reduction of fumarate, pyruvate, and CO_2 in *Shewanella oneidensis*. The predominant reaction is selected by the experimental conditions, and the results allow rational development of cell-based strategies to harness nature's intrinsic catalytic diversity for selective light-driven synthesis of a wide range of products.

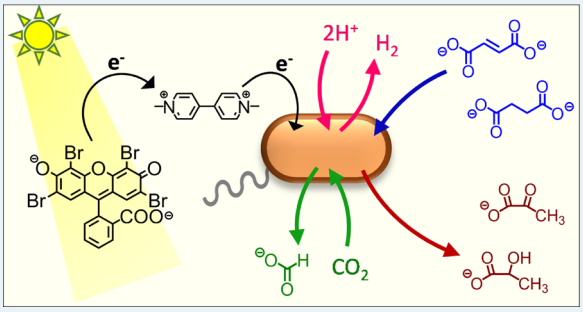

KEYWORDS: *proton reduction, CO_2 reduction, photocatalysis, hydrogenase, formate dehydrogenase, visible light*

INTRODUCTION

Photovoltaics provide scalable and cost-efficient conversion of solar energy to electricity and the inspiration for developing equally effective routes to solar chemicals for a sustainable society. An example for such processes is natural photosynthesis, but as it is primarily designed to convert CO_2 to sugars, this process presents several challenges for controlled generation of additional products. An example of contemporary interest is solar H_2 production through water splitting.[1−4] Certain algae and cyanobacteria can deliver photoenergized electrons from oxygenic, plantlike photosynthesis to hydrogenase enzymes that catalyze H_2 evolution from water (eq 1; all potentials are given vs SHE).

$$2H^+ + 2e^- \leftrightarrow H_2 \quad E_m = -420\ \text{mV},\ \text{pH}\ 7 \tag{1}$$

However, scalable solutions to biological H_2 production by this route have yet to be demonstrated, due to typical requirements of anaerobicity, sulfur deprivation, and the absence of CO_2. Furthermore, the process shares drawbacks with other routes to developing natural photosynthesis for solar chemicals production such as inefficient energy conversion[5] and reducing equivalents partitioned across competing metabolic pathways.[6]

To address these challenges, it is attractive to consider the oxidative and reductive half-reactions in isolation and the possible advantages of combining biotic and abiotic materials for photocatalysis. For example, abiotic photosensitizers can improve on Photosystems I and II as light-harvesting components by offering increased absorption across the incident solar spectrum, effective charge separation, and

Received: August 13, 2017
Revised: September 18, 2017
Published: September 19, 2017

DOI: 10.1021/acscatal.7b02736
ACS Catal. 2017, 7, 7558−7566

photosensitizer longevity.[7−10] However, enzymes remain attractive renewable electrocatalysts[11−13] and often deliver performances that match, or exceed, those of their best abiotic counterparts.[14−17] As a consequence, molecular dyes, (nanostructured) semiconductors, and quantum dots have been widely employed to deliver photoenergized electrons to purified enzymes for photocatalysis.[12,18−23] Nevertheless, there are significant bottlenecks to delivering scalable solar-driven synthesis by such approaches. Enzyme purification can be costly and time consuming, whereas methods to overcome the limited stability of the purified materials, for example through their covalent attachment to solid materials,[24,25] may be necessary. In seeking to harness nature's wide-ranging catalytic diversity to meet societal needs, there are many opportunities to evaluate alternate and ideally more versatile approaches.

Protein purification is avoided through the use of cell-based systems. For example, acetate was produced from CO_2 and sunlight using *Moorella thermoacetica*[26,27] with self-generated CdS nanoparticles as photosensitizers. Similarly, catalytic monooxygenation was achieved by delivering photoenergized electrons from the organic dye eosin Y to a P450 heme domain introduced into *Escherichia coli*.[28] Motivated by these examples, we reasoned that it should be possible to develop cell-based strategies affording selective access to a wide product range. A single microorganism would serve as a multifaceted catalyst with a repertoire defined by its intrinsic, or genetically enhanced, complement of enzymes and the light-driven reaction selected by user-defined conditions.

Here we demonstrate this concept for the nonphotosynthetic γ-proteobacterium *Shewanella oneidensis* MR-1 (MR-1) (Figure 1a). Methylviologen (MV, $E_m \approx -440$ mV,[29] pH 7) shuttles electrons from water-compatible photosensitizers to enzymes in MR-1 that catalyze four transformations of current interest: namely, H_2 evolution (eq 1), fumarate reduction as an example of C═C bond hydrogenation (eq 2), and the reductions of pyruvate and CO_2 as examples of C═O bond hydrogenation (eqs 3 and 4).

$$\text{fumarate} + 2e^- + 2H^+ \leftrightarrow \text{succinate} \quad E_m = +31 \text{ mV, pH 7} \tag{2}$$

$$\text{pyruvate} + 2e^- + 2H^+ \leftrightarrow \text{lactate} \quad E_m = -185 \text{ mV, pH 7} \tag{3}$$

$$CO_2 + 2e^- + H^+ \leftrightarrow HCO_2^- \quad E_m = -420 \text{ mV, pH 7} \tag{4}$$

Notably, photocatalysis is not dependent on the presence of outer membrane spanning porin:cytochrome (Mtr) complexes of MR-1 that can facilitate electron exchange between extra- and intracellular redox couples.[30−32] Instead, light-driven chemistry is underpinned by the well-described[16,33−35] abilities of MV to permeate cells and deliver electrons to numerous enzymes such that we envisage this strategy providing a versatile route to accessing a diversity of products from enzymes in numerous microbial species and genetically engineered strains. Our quantitative assessment of the determinants of light-driven synthesis provides a framework for the rational development of this strategy to access a selectable product range with control of product distribution.

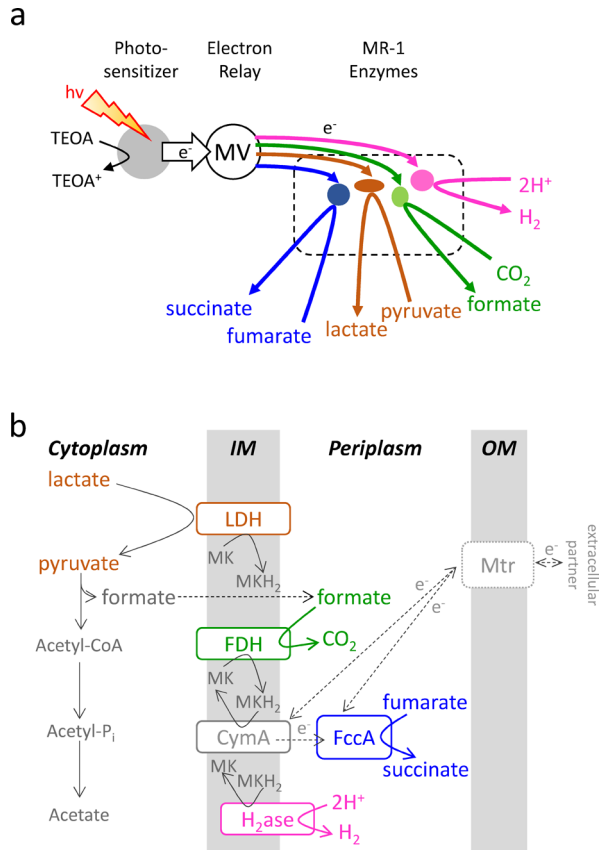

Figure 1. Cell-based photocatalysis by *S. oneidensis* MR-1. (a) Schematic of the strategy for MR-1-dependent photocatalytic reduction of protons, CO_2, fumarate, or pyruvate. Methylviologen (MV) relays electrons to MR-1 enzymes from abiotic photosensitizers with triethanolamine (TEOA) as a sacrificial electron donor. (b) Key MR-1 enzymes relevant to this study and anaerobic respiration by lactate oxidation coupled to the reduction of fumarate or protons (see text for details). Enzymes are lactate dehydrogenase (LDH), formate dehydrogenase (FDH), fumarate reductase (FccA), the [NiFe]- and [FeFe]-hydrogenases (H_2ase), and porin:cytochrome complexes (Mtr). IM denotes the inner membrane, OM the outer membrane, and MK menaquinone.

RESULTS AND DISCUSSION

Our findings are presented in the following order. First we demonstrate MR-1 can be cultured to support the four targeted transformations (eqs 1−4). Then we identify photosensitizers and sacrificial electron donors that allow photoreduction of MV^{2+} under conditions compatible with MR-1 catalysis. Finally we present quantitative analysis of MV-dependent light-driven chemical transformations by MR-1. Unless stated otherwise, experiments were performed in anaerobic solutions of 50 mM HEPES, 50 mM NaCl at pH 7. Reduction of CO_2 was investigated in solutions of dissolved sodium carbonate, and for simplicity the term "CO_2" is used to include the HCO_3^-, H_2CO_3, and dissolved CO_2 present in the equilibrated solutions. Quantification of product (substrate) is given in nanomoles to aid comparison across experiments designed to probe dissolved and gaseous species as described; full details can be found in the Supporting Information.

MR-1 Supports Chemically Driven Reduction of Protons, Fumarate, Pyruvate, and CO_2. Our approach to delivering cell-based photocatalytic production of multiple chemicals was informed by the metabolic capabilities of MR-1

DOI: 10.1021/acscatal.7b02736
ACS Catal. 2017, 7, 7558−7566

(Figure 1b). This bacterium has [NiFe]- and [FeFe]-hydrogenases[36−38] and catalyzes pyruvate reduction by the action of lactate dehydrogenase,[39,40] fumarate reduction by flavocytochrome c_3,[41] and formate oxidation by formate dehydrogenases.[42] While the reverse of the latter reaction, CO_2 reduction, has not to our knowledge been reported for MR-1, there is precedent from the behavior of homologous enzymes[16,43,44] that this chemistry may be possible.

As outlined in Figure 1b, MR-1 can grow anaerobically when oxidation of the electron donor lactate to acetate and CO_2 is coupled to reduction of the terminal electron acceptor fumarate to succinate.[39,42] Lactate oxidation becomes coupled to proton reduction upon depletion of fumarate during acceptor-limited growth.[36−38] As a consequence, and with the aim to produce MR-1 containing enzymes active toward the four desired transformations, an inoculum (2% v/v) of MR-1 was introduced to Hungate tubes that contained M72 medium (see Methods in the Supporting Information) with 37.5 mM lactate as the electron donor and 18.8 mM fumarate as the electron acceptor (10 mL media, 7 mL headspace of N_2). Growth of the cultures was monitored spectrophotometrically at 590 nm ($OD_{590\,nm}$), and headspace H_2 was analyzed by gas chromatography (Figure 2a). There was no evidence for H_2 production in parallel experiments that omitted MR-1 or used a strain[45] ($HydA^-/HyaB^-$) without functional hydrogenases (Figure 2a). It was concluded that MR-1 contained active hydrogenases after culture for at least 18 h under the selected conditions.

Sodium dithionite, a chemical reductant that readily reduces MV^{2+} to MV^+, was used to assess whether MV^+ would reduce the MR-1 hydrogenases. Sodium dithionite was added to samples containing MV and MR-1 grown for 24 h as described above, harvested anaerobically, and resuspended in the desired solution to $OD_{590\,nm} \approx 0.25$ (equivalent to ∼0.17 mg of protein mL^{-1}). A H_2-sensing electrode in the sample reported an accumulation of 725 ± 97 nmol of H_2 over 30 min (Figure 2b). Without MV there was 60-fold less H_2 (Figure 2b), revealing MV to be an effective facilitator of electron transfer to MR-1 hydrogenases.

The activity of MR-1 toward fumarate reduction was assessed by 30 min incubation of cells ($OD_{590\,nm} \approx 0.25$, 1 mL), MV (0.5 mM), and sodium dithionite (0.8 mg mL^{-1}) with sodium fumarate (∼4700 nmol). After the cells had been pelleted by centrifugation, the supernatant was removed and analyzed by ^1H NMR spectroscopy. The presence of succinate at ∼3800 nmol and fumarate at ∼600 nmol revealed that the desired reaction had occurred (Table S1 and Figure S1 in the Supporting Information). An equivalent experiment with pyruvate (∼2200 nmol) in place of fumarate demonstrated formation of lactate (∼900 nmol) with pyruvate consumption (Table S1). Formate (∼1500 nmol) was produced when MR-1 was incubated with CO_2 (∼5000 nmol) (Table S1). Thus, MR-1 cultured under our chosen conditions catalyzed all four reactions of interest: namely, the reduction of protons, fumarate, pyruvate, and CO_2 to, respectively, H_2, succinate, lactate, and formate.

Light-Driven Production of MV^+ in Conditions Compatible with MR-1 Biocatalysis. Our strategy for cell-based photocatalysis requires effective transfer of photoenergized electrons to a number of MR-1 enzymes (Figure 1a). The ability of MV to permeate bacterial cells and deliver electrons from chemical reductants to numerous enzymes is well-documented and the basis of many biochemical assays.[16,33−35] This property of MV mediates electron exchange between bacteria and electrodes in microbial fuel cells.[46,47] In addition, water-compatible dyes[34,35,48−51] are reported to photoreduce MV^{2+} to MV^+, and MV has been shown to support photocatalytic H_2 production by relaying electrons from TiO_2 and Bi_2O_3 semiconductor particles to hydrogenases inside *E. coli*,[52−54] *Rhodopseudomonas capsulate*,[50] and *Clostridium butyricum*.[55] Here, we confirmed the photocatalytic reduction of MV^{2+} under conditions where MR-1 performed the four desired chemical transformations by representatives of three classes of photosensitizer: an acridine dye proflavine,[48] the xanthene dyes eosin Y[49] and fluorescein,[50] and the inorganic complexes $Ru(bpy)_3^{2+}$ (bpy = 2,2′-bipyridine)[51] and $Ru(bpy)_2(4,4'\text{-}(PO_3H_2)_2bpy)^{2+}$ (RuP).[56,57] Structures and

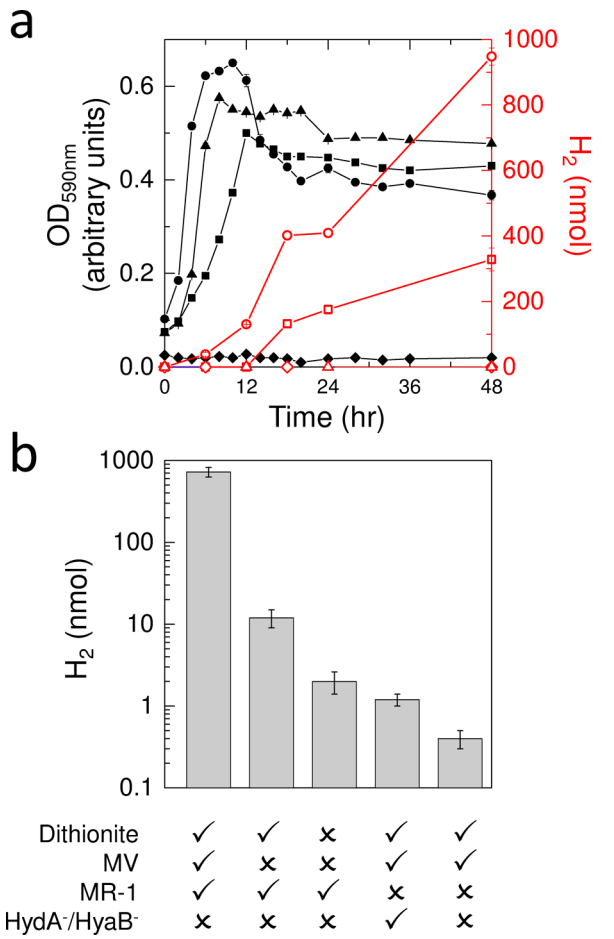

Figure 2. Hydrogenase activity of MR-1. (a) Growth curves (black) and headspace H_2 (red) for MR-1 (squares), $HydA^-/HyaB^-$ (triangles), Mtr^- (circles), or no bacteria (diamonds). Inoculation was at 0 h of media (10 mL) with 37.5 mM lactate and 18.8 mM fumarate. Samples had 7 mL headspace (100% N_2 at inoculation). Optical densities ($OD_{590\,nm}$) are mean values ($n = 4$), and the majority of error bars with standard error are too small to resolve. Headspace H_2 mean values ($n = 2$) are given; error bars indicate maximum and minimum. Lines serve as a guide to the eye. (b) Dissolved H_2 in anaerobic suspensions of MR-1 or $HydA^-/HyaB^-$ ($OD_{590\,nm} \approx 0.25$ for 1.29 mL volume with negligible headspace) 30 min after addition of dithionite (0.3 mg mL^{-1}) and/or MV (0.3 mM) as indicated in 50 mM HEPES, 50 mM NaCl, pH 7. Mean values with standard error from five biological replicates for MR-1, dithionite, and MV are given. Other values are means from two biological replicates; error bars indicate maximum and minimum.

DOI: 10.1021/acscatal.7b02736
ACS Catal. 2017, 7, 7558−7566

spectral properties of these molecules are presented in Figure S2 and Table S2 in the Supporting Information.

The ability of the selected dyes to photoreduce colorless MV^{2+} to blue MV^{+} was assessed by electronic absorption spectroscopy after 10 min exposure to visible light (0.7 kW m^{-2}, see Methods and Figure S3 in the Supporting Information) in the presence of triethanolamine (TEOA, E_m ≈ +820 mV,[58] pH 7) as a sacrificial electron donor (Figure 3).

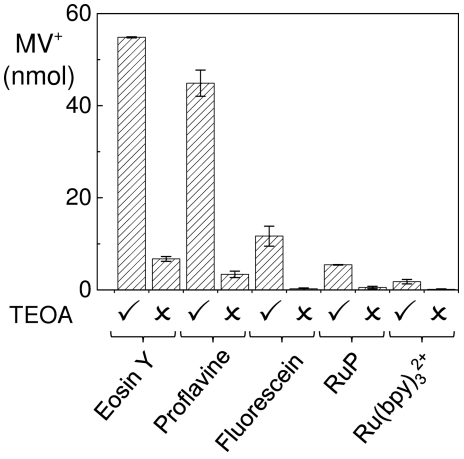

Figure 3. Photoreduction of MV by xanthene, acridine, and Ru(II) dyes. MV^{+} was quantified after 10 min irradiation (0.7 kW m^{-2}) of MV^{2+} (0.061 mM) with the indicated photosensitizer (0.02 mM) in the presence or absence of TEOA (12 mM) as a sacrificial electron donor. Anaerobic samples (1 mL volume) with 50 mM HEPES, 50 mM NaCl, pH 7. The path length was 1 cm. Mean values (n = 2) are given; error bars indicate maximum and minimum.

The rate of MV^{+} formation was dependent on photosensitizer and decreased in the order eosin Y > proflavine > fluorescein > RuP > $Ru(bpy)_3^{2+}$ (Figure 3). Replacing TEOA by other established sacrificial electron donors[59] photogenerated less MV^{+} (Figure S3). As a consequence and unless stated otherwise, TEOA was included in the experiments described below that quantified photocatalysis by MR-1.

Quenching of a photosensitizer excited state (PS*) can occur by two pathways (Figure S4a in the Supporting Information). For reductive quenching PS* oxidizes TEOA; this forms PS^{-}, which can then reduce MV^{2+} to MV^{+} and in the process regenerate PS^{0}. For oxidative quenching PS* reduces MV^{2+} to MV^{+}; this forms PS^{+}, which can then oxidize TEOA to re-form PS^{0}. To gain insight into the mechanism(s) operating under our conditions, fluorescence intensity was assessed as a function of the concentration of TEOA or MV^{2+} (Figure S4b). For all photosensitizers the Stern–Volmer plots revealed MV^{2+} to be a more effective quencher than TEOA. Why then is photoproduction of MV^{+} (Figure 3) greater in the presence than in the absence of TEOA? Making the reasonable assumption that fluorescence quenching arises from electron transfer and noting that the $PS^{+/0}$ couples are >+900 mV (Table S2 in the Supporting Information), we can explain this observation if PS^{+}, generated by oxidative quenching with MV^{+} formation, is returned to PS^{0} by oxidation of excess TEOA rather than MV^{+} (Figure S4a). The Stern–Volmer plots fail to provide immediate insight into the relative extents of MV^{+} photoproduction by the PS studied, for which a full description requires resolution of multiple electron transfer rates (Figure S4a) and appropriate consideration of the spectral properties of each photosensitizer and the incident light.

Light-Driven H_2 Evolution by MR-1. Visible-light-driven H_2 production by MR-1 was quantified by a H_2-sensing electrode placed in a sealed, anaerobic, and transparent (wavelengths >400 nm) glass vessel filled with an anaerobic cell suspension (1.7 mL, $OD_{590\,nm}$ ≈ 0.25): i.e., there was negligible headspace. H_2 accumulated in irradiated suspensions containing MV and a photosensitizer (Figure 4). As is usual for

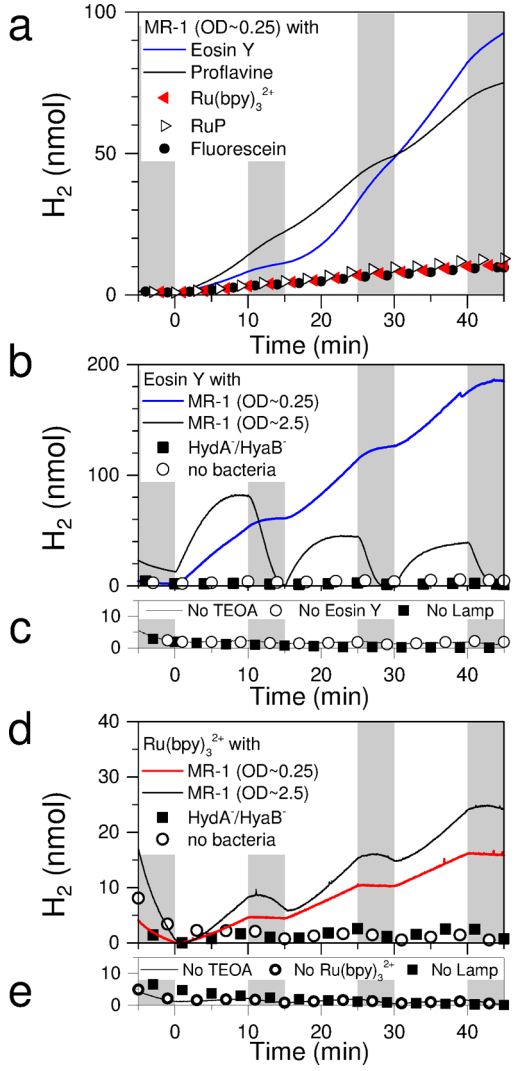

Figure 4. Light-driven H_2 production by MR-1. Samples experienced ambient light throughout and irradiation by visible light at 0.7 kW m^{-2} between 0 and 10, 15 and 25, and 30 and 40 min (white panels). (a) MR-1 suspensions ($OD_{590\,nm}$ ≈ 0.25) with the indicated photosensitizers (0.11 mM), TEOA (60 mM), and MV (0.3 mM). (b) Suspensions of MR-1 ($OD_{590\,nm}$ ≈ 0.25 or 2.5 as indicated) and $HydA^{-}/HyaB^{-}$ ($OD_{590\,nm}$ ≈ 0.25) with eosin Y (0.11 mM), TEOA (60 mM), and MV (0.3 mM). (c) As for the blue line in (b) except for the omission of TEOA, eosin Y, or irradiation at 0.7 kW m^{-2} as indicated. (d) Suspensions of MR-1 ($OD_{590\,nm}$ ≈ 0.25 or 2.5 as indicated) and $HydA^{-}/HyaB^{-}$ ($OD_{590\,nm}$ ≈ 0.25) with $Ru(bpy)_3^{2+}$ (0.11 mM), TEOA (60 mM), and MV (0.3 mM). (e) As for the red line in (d) except for the omission of TEOA, $Ru(bpy)_3^{2+}$, or irradiation at 0.7 kW m^{-2} as indicated. Anaerobic samples (1.7 mL volume, negligible headspace) contained 50 mM HEPES, 50 mM NaCl at pH 7 and 23 °C. Different MR-1 cultures were aliquoted for the experiments of (a), of (b, c), and of (d, e) (see text for details).

DOI: 10.1021/acscatal.7b02736
ACS Catal. 2017, 7, 7558–7566

studies with biological samples, the use of cells from separate cultures produced some variation (<3-fold) in the absolute amount of product for a given condition (e.g. Figure S5 in the Supporting Information). Nevertheless, and most significantly for the work presented here, the H_2 generated varied in a reproducible manner with changes in experimental parameters as described below.

Effect of Photosensitizer Identity. The nature of the photosensitizer was found to have a decisive effect on the amount of H_2 produced (e.g., Figure 4a). Eosin Y and proflavine supported most H_2 production. Fluorescein, Ru(bpy)$_3^{2+}$, and RuP generated 7-fold less H_2, in accord with the relative effectiveness of these photosensitizers for MV^{2+} photoreduction (Figure 3). No detectable H_2 was produced when photosensitizer, irradiation, or TEOA was omitted (e.g. Figure 4c,e) or when MR-1 was omitted or replaced by the $HydA^-/HyaB^-$ strain (e.g. Figure 4b,d). Omission of MV, discussed further below, also led to no detectable H_2 production (e.g., Figure 5). Taken together, these observations demonstrate light-driven H_2 evolution by MR-1 hydrogenases using the selected photosensitizers with MV as electron relay and TEOA as sacrificial electron donor (Figure 1a).

Effect of MR-1 Cell Density. Further insight into rate-defining features of light-driven H_2 production was gained with eosin Y and Ru(bpy)$_3^{2+}$ as representative photosensitizers. The first series of experiments assessed the effect of a 10-fold increase of MR-1 cell density in samples exposed to periodic irradiation at 0.7 kW m^{-2} (Figure 4b,d). As discussed below, over the 45 min experiment H_2 accumulated in all of the samples except that of the higher density MR-1 suspension with eosin Y (Figure 4b,d).

For both photosensitizers the 10-fold increase in cell density led to a 1.5-fold increase in the rate of H_2 evolution during the first 10 min of irradiation (Figure 4b,d, 0 to 10 min). This is significantly less than the 10-fold increase expected if hydrogenase activity contributed to the rate-defining step(s) of H_2 evolution, a point we discuss further in the next section. When the light source was removed, the dissolved H_2 decreased for the higher density cell suspensions (Figure 4b,d, 10 to 15 min), and this was particularly pronounced with eosin Y, where the dissolved H_2 fell below a detectable level. As hydrogenases are reversible enzymes,[60] this behavior is most likely due to H_2 oxidation coupled to the reduction of MR-1 enzymes and metabolites. Why this effect was more pronounced with eosin Y than with Ru(bpy)$_3^{2+}$ is not apparent, but these patterns were repeated during two further cycles of exposure to irradiation at 0.7 kW m^{-2}. Over successive cycles of irradiation it was also noted that less H_2 was produced with eosin Y in the higher density cell suspension (Figure 4b). This may be an indication that this photosensitizer is more susceptible to photodamage in these conditions (see below).

Rate-Defining Events in H_2 Production. In view of the results above, the H_2 produced in response to changes in light intensity, pH, or MV concentration was investigated with MR-1 suspensions of $OD_{590\,nm} \approx 0.25$ irradiated continuously for 30 min (Figure 5). Lower intensity light produced less H_2. The pH dependence of H_2 production with eosin Y was opposite to that with Ru(bpy)$_3^{2+}$. For both dyes the changes were small despite hydrogenases typically[60] evolving H_2 more rapidly at pH 6 than at pH 8 and neither dye changing protonation state[61] in this pH range. H_2 production did not scale linearly with MV concentration. The highest MV concentration will favor reduction of PS^+ by oxidation of MV^+ rather than TEOA

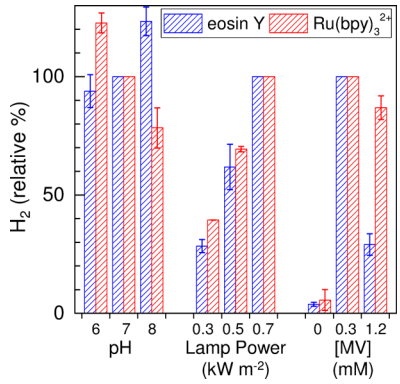

Figure 5. Effect of pH, lamp power, and MV concentration on light-driven H_2 production by MR-1. Dissolved H_2 was determined after 30 min irradiation of gently stirred MR-1 suspensions ($OD_{590\,nm} \approx 0.25$) with eosin Y or Ru(bpy)$_3^{2+}$ (0.11 mM). The light intensity was 0.7 kW m^{-2}, at pH 7 with MV present at 0.3 mM unless stated otherwise. Mean values are given for two biological replicates; error bars indicate maximum and minimum. Values are normalized to the mean with 0.3 mM MV, pH 7 irradiated at 0.7 kW m^{-2} for each photosensitizer where dissolved H_2 was 33 ± 5 nmol with Ru(bpy)$_3^{2+}$ (n = 5) and 242 ± 24 nmol with eosin Y (n = 6). Anaerobic samples (1.65 mL volume, negligible headspace) were used with TEOA (60 mM) in 50 mM HEPES, 50 mM NaCl at 23 °C.

(see above), without leading to H_2 production. Very little H_2 was produced in the absence of the MV electron shuttle. These observations, in agreement with those presented above, point to the rate-limiting event(s) of H_2 production involving photosensitizer and MV. Given the previously reported ability of eosin Y to act as an intracellular photosensitizer in *E. coli*[28] and to deliver photoenergized electrons directly to *Desulfomicrobium baculatum* [NiFeSe]-hydrogenase,[62] the requirement for MV to support eosin Y dependent light-driven chemistry in our system is notable. Clearly the requirements for electron delivery to the MR-1 hydrogenases in this cell-based system are more complex than might be inferred from those previous reports.

It is well-established that MV can enter Gram-negative bacteria[63] such as MR-1. However, electrons can also enter MR-1 through porin:cytochrome complexes[30−32] that span the bacterial outer membrane (Figure 1b). The most prevalent of these complexes, MtrCAB, was revealed in our samples when proteins were resolved by SDS-PAGE and visualized by immunoblotting (Figure S6 in the Supporting Information). An MR-1 strain[64] (Mtr^-) lacking MtrCAB and the paralog MtrDEF was studied to assess whether these complexes were critical for light-driven H_2 production. The Mtr^- strain grew faster and produced more H_2 than MR-1 (Figure 2a), and immunoblots failed to detect MtrCAB in harvested Mtr^- (Figure S6a). The enhanced H_2 production may be due to Mtr^- having approximately twice the hydrogenase activity of MR-1 (Figure S6b), although increased electron delivery to the hydrogenases in the absence of a reservoir for electrons provided by the hemes of the Mtr complexes is also possible. Nevertheless, light-driven H_2 production with both eosin Y and Ru(bpy)$_3^{2+}$ was comparable to that by MR-1 (Figure S6c). Thus, light-driven H_2 evolution was not dependent on the presence of MtrCAB or MtrDEF complexes in the MR-1 outer membrane and it is likely that MV enters the periplasm to pass electrons to hydrogenases (Figure 1a).

DOI: 10.1021/acscatal.7b02736
ACS Catal. 2017, 7, 7558−7566

Sustained H_2 Production. The conditions of our studies were chosen for their experimental tractability rather than MR-1 viability: for example, no substrates for growth or cell maintenance reactions were included. Indeed, cells pelleted after 30 min irradiation (0.7 kW m^{-2}) with TEOA, MV, and eosin Y or $Ru(bpy)_3^{2+}$ contained respectively no detectable and 77 colony-forming units (CFU) mL^{-1}. Equivalent MR-1 suspensions incubated in the dark contained ~6 × 10^4 CFU mL^{-1}, whereas ~7 × 10^7 CFU mL^{-1} was recovered from suspensions irradiated in the absence of photosensitizers, MV, and TEOA. Thus, it appears that electron flow due to irradiation enhances the toxicity of the chemicals required for photocatalysis, which may relate to methylviologen (paraquat) induced stress response(s) in MR-1[65] that can lead to cell death. Nevertheless, it was of interest to build on the results presented above with the aim to improve photocatalytic H_2 production. To this end a N_2-filled headspace (3.35 mL) was introduced into which H_2 could escape from the cell suspension (1.65 mL) and headspace H_2 was quantified over a period of 4 days of irradiation (Figure 6a). Equivalent irradiation (0.02 kW m^{-2}) of the necessary number of samples was ensured by use of a photosynthetic growth chamber (see Methods in the Supporting Information).

Eosin Y supported significantly more H_2 production in the first 24 h irradiation than $Ru(bpy)_3^{2+}$ (Figure 6a), in accord with the behavior described above (Figure 3). When illumination of the MR-1 suspensions was continued beyond 24 h, the H_2 content rose steadily with $Ru(bpy)_3^{2+}$ but diminished with eosin Y and after 4 days both samples contained equivalent levels of H_2. Hydrogenase activity quantified for the resuspended cellular materials collected after centrifugation, and the supernatants, showed that active enzyme was primarily associated with the cellular material and varied little over the course of the experiment (Figure 6b). It is evident that the hydrogenases remain active during the 4 days of irradiation, and this matches the longest-lived system we are aware of with purified hydrogenase[66] aside from cases where longevity has been increased by covalent attachment to an electrode.[24,25] The sustained H_2 production seen with $Ru(bpy)_3^{2+}$ is most likely due to its being less susceptible to photodamage than eosin Y.[67] Photodamage of eosin Y will remove the driving force for H_2 evolution such that the loss of H_2 after 24 h irradiation of that sample may be due to slow leakage of H_2 from the vessel or H_2 oxidation coupled to reduction of cellular enzymes and metabolites as described above.

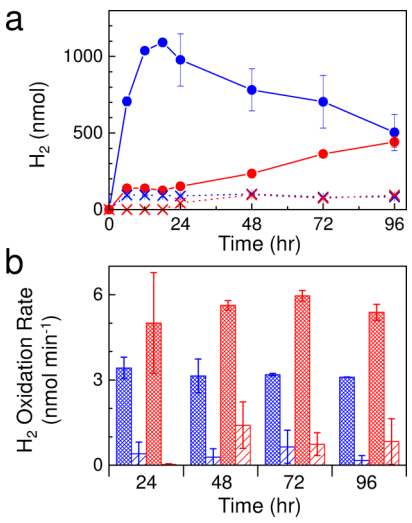

Figure 6. Properties of MR-1 suspensions over 4 days of irradiation by visible light (0.02 kW m^{-2}) with eosin Y (blue) or $Ru(bpy)_3^{2+}$ (red). (a) Headspace H_2 (circles) for anaerobic suspensions ($OD_{590\,nm}$ ≈ 0.25 in 1.65 mL volume with 3.35 mL headspace) containing photosensitizer (0.11 mM), MV (0.3 mM), and TEOA (60 mM) in 50 mM HEPES, 50 mM NaCl, pH 7 at 25 °C. Mean values (symbols) with lines given as a guide to the eye; for 6−18 h n = 2 (technical replicates), error bars indicate maximum and minimum; for 0 and 24−96 h mean values ($n \geq 5$ with ≥3 biological replicates) are given with standard error. Headspace H_2 (crosses) values are given for parallel experiments without MR-1 (mean values from technical duplicates, error bars indicate maximum and minimum). (b) Initial rates of H_2 oxidation coupled to benzylviologen reduction by cell pellets (darker bars) and supernatants (lighter bars) recovered after centrifugation of MR-1 suspensions irradiated with eosin Y (blue) or $Ru(bpy)_3^{2+}$ (red) as described in (a). Mean values are given for two biological replicates; error bars indicate maximum and minimum.

The apparent quantum efficiency for H_2 production was defined under irradiation (0.01 kW m^{-2}) as [2 × (number of H_2 molecules produced)]/(number of incident photons). MR-1 suspensions were irradiated at 500 or 450 nm with eosin Y or $Ru(bpy)_3^{2+}$, respectively, and the headspaces were sampled after 1 h (see Methods in the Supporting Information). Under these conditions the apparent quantum efficiencies for eosin Y and $Ru(bpy)_3^{2+}$ were 0.6 ± 0.1% and 0.5 ± 0.1%, respectively, and we note that these values represent lower limits for photocatalysis, due to the assumption that all of the light is harvested by the photosensitizer-containing MR-1 suspension. Photoproduction of MV^+ in the absence of MR-1 but otherwise equivalent conditions occurred with an apparent quantum efficiency of 2.1 ± 0.2% for eosin Y and 1.0 ± 0.1% for $Ru(bpy)_3^{2+}$, where the efficiency is defined as (number of molecules of MV^+ produced)/(number of incident photons). It can be concluded that for both photosensitizers the primary bottleneck to more efficient photocatalytic H_2 production is transfer of photoexcited electrons to MV^{2+}, rather than the delivery of electrons from MV^+ to the hydrogenases. We note that, during irradiation with white light, significantly greater photoproduction of H_2 with eosin Y than with $Ru(bpy)_3^{2+}$ can be explained by the former having greater extinction coefficients at wavelengths for which the incident light has greater instensity (Figure S2 and Table S2 in the Supporting Information).

Light-Driven C═C and C═O Bond Hydrogenation by MR-1. Given the efficiency with which MV^+ transferred photogenerated electrons to hydrogenases, it was of interest to assess whether these electrons could be delivered to enzymes that catalyze the reduction of C-based substrates. The superior H_2 production achieved with 0.11 mM eosin Y, 0.3 mM MV, and an MR-1 suspension of $OD_{590\,nm}$ ≈ 0.25 made these the conditions of choice for such investigations. H_2 production over 30 min irradiation (0.7 kW m^{-2}) was significantly diminished by the presence of fumarate, pyruvate, or CO_2 (Figure 7a), consistent with the diversion of photoenergized electrons to enzymes catalyzing the reduction of the C-based substrates. Confirmation of, and greater insight into, this behavior was afforded by NMR analysis of replicate samples that were best obtained from 24 h irradiation (0.02 kW m^{-2}) in a photosynthetic growth chamber (see above and Methods in the Supporting Information).

DOI: 10.1021/acscatal.7b02736
ACS Catal. 2017, 7, 7558−7566

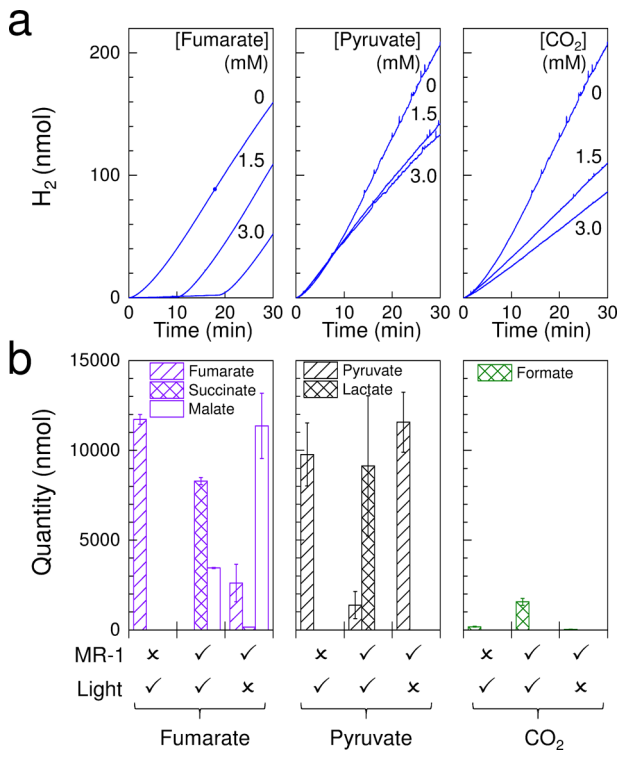

Figure 7. Light-driven reduction of fumarate, pyruvate, and CO_2 by MR-1. (a) Dissolved H_2 in gently stirred MR-1 suspensions ($OD_{590\,nm}$ ≈ 0.25 for 1.29 mL volume with negligible headspace) with eosin Y (0.11 mM), TEOA (60 mM), MV (0.3 mM), and the indicated concentrations of fumarate (left), pyruvate (middle), or CO_2 (right). Irradiation was at 0.7 kW m^{-2} throughout. All samples were anaerobic in 50 mM HEPES, 50 mM NaCl, pH 7 at 23 °C. (b) Composition of supernatants recovered from samples incubated for 24 h with eosin Y (0.08 mM), MV (0.5 mM), TEOA (50 mM), and 10 mM fumarate (left), pyruvate (middle), or CO_2 (right). Assays were performed with or without MR-1 ($OD_{590\,nm}$ ≈ 0.25) in the dark or irradiated (~0.02 kW m^{-2}). Mean values are given from technical duplicates; error bars indicate maximum and minimum. All samples were anaerobic in 50 mM HEPES, 50 mM NaCl, pH 7 at 25 °C.

^{1}H NMR data for MR-1 irradiated in the presence of ~9800 nmol of pyruvate revealed almost complete conversion to lactate (~9100 nmol, 93% yield) with no evidence for generation of additional products or dark reactions (Figure 7b and Table S3 and Figure S7 in the Supporting Information). Irradiation in the presence of ~11700 nmol of fumarate produced succinate (~8300 nmol, 70% yield) as the major product and malate (~3500 nmol, 30% yield) as the minor product. Dark incubated MR-1 hydrolyzed fumarate to malate (~11400 nmol, 100% yield) in a reaction catalyzed by fumarase (SO_2222). That significantly less malate is present after 24 h irradiation illustrates the scope of light-driven chemistry to exert temporal control over the progress of a reaction through the imposition of a persistent driving force to ensure the availability of reducing equivalents. It is also of note that the time courses (Figure 7a) for H_2 evolution with 1.5 and 3 mM fumarate show no detectable H_2 production for the first 10 or 20 min of irradiation, respectively. This makes it reasonable to assume that the majority of fumarate is consumed prior to H_2 production such that the Coulombic efficiency for fumarate reduction need not be sacrificed by using MV to deliver photoenergized electrons to microorganisms containing hydrogenases. The average rate of fumarate reduction is on the order of 250 nmol min^{-1}, whereas in the absence of carbon substrates, H_2 is produced at a rate of 4 nmol min^{-1}. We anticipate that an appropriate choice of conditions would secure complete conversion of fumarate to succinate: i.e., without malate production and with high Coulombic efficiency.

The ^{1}H NMR data for MR-1 irradiated with ~10000 nmol of CO_2 revealed ~1600 nmol of formate (16% yield) (Figure 7b and Table S3 and Figure S7 in the Supporting Information). ^{13}C NMR analysis of equivalent experiments with ^{13}C-CO_2 revealed similar levels of ^{13}C-formate (~1790 nmol, 18% yield), and parallel samples kept in the dark contained no detectable ^{13}C-formate (Figure S8 in the Supporting Information). Given that the time courses for H_2 production over 30 min (Figure 7a) revealed CO_2 reduction to be as effective as pyruvate reduction in competing with hydrogenases for photoenergized electrons, these yields of formate were lower than expected. Dissolution of CO_2 or the compulsory involvement of H_2 as an intermediate in CO_2 reduction, such as would occur with a formate–hydrogen lyase complex, is unlikely to cause this behavior, as only 3-fold more formate was observed after minimizing the sample headspace or replacing MR-1 with the $HydA^-/HyaB^-$ strain. The lower than anticipated amount of formate may indicate that enzymatic conversion to other products occurs or that the pathway leading to CO_2 reduction is less stable under prolonged irradiation than those reducing protons, fumarate, and pyruvate.

Finally we note that the H_2 evolution time courses of Figure 7a reveal that light-driven fumarate reduction is significantly faster than reduction of protons, pyruvate, and CO_2. This may reflect the high cellular abundance of the soluble, periplasmic fumarate reductase that has surface-exposed redox cofactors.[68] The hydrogenases,[36−38] formate dehydrogenases,[42] and lactate dehydrogenases[39,40] are membrane associated and exchange electrons primarily with the Q-pool such that they may receive electrons from MV^+ via the electron transfer properties of intermediary enzymes.

Prospects for Whole-Cell Photocatalytic Production of Multiple, Selected Chemicals. The results presented here demonstrate the ability of MV to transfer photogenerated electrons to multiple enzymes for cell-based photocatalytic production of a selectable product range. The apparent quantum efficiencies are low (~0.5%) and primarily limited by photoreduction of MV^{2+}, and similar behavior was noted[53] for MV-dependent H_2 production by *E. coli* irradiated with anatase TiO_2 as a photosensitizer. While the present work was under review, Honda et al. reported[54] that replacing the anatase with P-25 TiO_2 improved the quantum efficiency for H_2 production to ~25%. As a consequence, given the promiscuity of MV as an electron relay to intracellular enzymes, we envisage similarly impressive quantum efficiencies for the production of multiple chemicals when MV is used in combination with photosensitizers optimized for MV^{2+} reduction.

For more sustainable whole-cell photocatalysis it is desirable to increase the longevity and decrease the complexity of the present systems. Ideally, the repair and regeneration machinery of living cells would be retained. Inclusion of cellular energy sources could help to achieve this but would increase the chemical complexity of the system. More benefit is likely to be gained by changing and/or simplifying the components required for sustaining the supply of photoenergized electrons. For example, TEOA has proved to be a successful sacrificial electron donor for the reductive half-reactions studied here but its one-electron-oxidation product is a potentially harmful

DOI: 10.1021/acscatal.7b02736
ACS Catal. 2017, 7, 7558−7566

radical species. Using a cathode or recycling oxidized ascorbate[69] with tris(carboxyethyl)phosphine would avoid generating such species.

Ultimately a system that delivers photoenergized electrons to enzymes inside bacteria without a requirement for MV would be preferable, since its substitution would avoid using a toxic and relatively costly, although regenerated, electron relay. Such a relay may be naturally produced[30] or be a membrane-permeable ferrocene such as DFSO+.[70] Alternatively, the photosensitizer could deliver electrons directly to a naturally occurring outer membrane spanning electron conduits; in this context it is significant that eosin Y, proflavine, and fluorescein were recently shown[71] to catalyze complete photoreduction of the purified outer membrane spanning the MtrCAB complex from MR-1. The present work illustrates how engaging these photosensitizers for direct light-driven catalysis by MR-1 via Mtr complexes is more challenging than predicted from the behavior of these dyes with purified MtrCAB. In the cellular context the targeted transformations may go undetected due to slow intracellular electron transfer from photoreduced Mtr complexes or the photosensitizers may be unable to reduce the extracellular cytochromes due to hindrance by lipopolysaccharides or nonproductive quenching of their excited states. These possibilities form the focus of continued experimentation in our laboratories, with the aim of developing cell-based systems as sustainable routes to access a wide product range.

CONCLUSIONS

In summary we have demonstrated light-driven H_2 evolution and the hydrogenation of the C═C bond in fumarate or the C═O bonds in pyruvate and CO_2 by a nonphotosynthetic microorganism. These transformations are achieved without enzyme purification by using MV to transfer photoenergized electrons from water-soluble dyes to the corresponding enzymes in a cell-based assay. Given the promiscuity of MV as a redox partner of enzymes in numerous microorganisms, our approach provides a versatile route to accessing diverse and selective visible-light-driven chemical syntheses without the need for costly enzyme purification.

ASSOCIATED CONTENT

Supporting Information

The Supporting Information is available free of charge on the ACS Publications website at DOI: 10.1021/acscatal.7b02736.

Materials and methods, representative NMR spectra, NMR-derived quantification of carbon substrates, photosensitizer structures, and absorbance maxima, spectral properties of irradiation sources and photosensitizers, methylviologen photoreduction with different photosensitizers and sacrificial electron donors, and hydrogenase activity and MtrCAB content of *Shewanella* strains (PDF)

AUTHOR INFORMATION

Corresponding Authors

*E-mail for L.J.C.J.: l.j.c.jeuken@leeds.ac.uk.
*E-mail for E.R.: reisner@ch.cam.ac.uk.
*E-mail for J.N.B.: j.butt@uea.ac.uk.

ORCID

Gwénaëlle Le Gall: 0000-0002-1379-2196
Lars J. C. Jeuken: 0000-0001-7810-3964
Erwin Reisner: 0000-0002-7781-1616
Julea N. Butt: 0000-0002-9624-5226

Notes

The authors declare no competing financial interest.

ACKNOWLEDGMENTS

Funding was obtained from the U.K. Biotechnology and Biological Sciences Research Council (grants BB/K009753/1, BB/K010220/1, BB/K009885/1, Doctoral Training Partnership Ph.D. studentship to S.F.R., and iCASE Ph.D. studentship to J.A.D.), the Engineering and Physical Sciences Research Council (EP/M001989/1; Ph.D. studentship 1307196 to E.V.A.), and a Royal Society Leverhulme Trust Senior Research Fellowship to J.N.B. We thank Mr. Jack Day for assistance with H_2 oxidation assays, Mr. Michael Norman for assistance with Western blotting, and Dr. Manuela A. Gross for providing a sample of RuP. We also thank Dr. Nikolay Kornienko for critical discussion of the manuscript and Dr. Moritz Kuehnel for assistance with measurement of quantum efficiencies.

ABBREVIATIONS

bpy, 2,2′-bipyridine; CFU, colony forming units; FDH, formate dehydrogenase; IM, inner membrane; LDH, lactate dehydrogenase; MK, menaquinone; MR-1, *Shewanella oneidensis* MR-1; MV, methyl viologen; $OD_{590\ nm}$, optical density at 590 nm; OM, outer membrane; RuP, $Ru(bpy)_2(4,4'\text{-}(PO_3H_2)_2bpy)^{2+}$; TEOA, triethanolamine

REFERENCES

(1) Lee, H.; Vermaas, W.; Rittmann, B. *Trends Biotechnol.* **2010**, *28*, 262−271.
(2) Tachibana, Y.; Vayssieres, L.; Durrant, J. *Nat. Photonics* **2012**, *6*, 511−518.
(3) Volgusheva, A.; Styring, S.; Mamedov, F. *Proc. Natl. Acad. Sci. U. S. A.* **2013**, *110*, 7223−7228.
(4) Ghirardi, M.; Posewitz, M.; Maness, P.; Dubini, A.; Yu, J.; Seibert, M. *Annu. Rev. Plant Biol.* **2007**, *58*, 71−91.
(5) Blankenship, R.; Tiede, D.; Barber, J.; Brudvig, G.; Fleming, G.; Ghirardi, M.; Gunner, M.; Junge, W.; Kramer, D.; Melis, A.; Moore, T.; Moser, C.; Nocera, D.; Nozik, A.; Ort, D.; Parson, W.; Prince, R.; Sayre, R. *Science* **2011**, *332*, 805−809.
(6) Michel, H. *Angew. Chem., Int. Ed.* **2012**, *51*, 2516−2518.
(7) Scholes, G.; Fleming, G.; Olaya-Castro, A.; van Grondelle, R. *Nat. Chem.* **2011**, *3*, 763−774.
(8) Frischmann, P.; Mahata, K.; Wurthner, F. *Chem. Soc. Rev.* **2013**, *42*, 1847−1870.
(9) Croce, R.; van Amerongen, H. *Nat. Chem. Biol.* **2014**, *10*, 492−501.
(10) Panda, M. K.; Ladomenou, K.; Coutsolelos, A. G. *Coord. Chem. Rev.* **2012**, *256*, 2601−2627.
(11) Cracknell, J.; Vincent, K.; Armstrong, F. *Chem. Rev.* **2008**, *108*, 2439−2461.
(12) Bren, K. *Interface Focus* **2015**, *5*, 20140091.
(13) Shi, J. F.; Jiang, Y. J.; Jiang, Z. Y.; Wang, X. Y.; Wang, X. L.; Zhang, S. H.; Han, P. P.; Yang, C. *Chem. Soc. Rev.* **2015**, *44*, 5981−6000.
(14) Jones, A. K.; Sillery, E.; Albracht, S. P. J.; Armstrong, F. A. *Chem. Commun.* **2002**, 866−867.
(15) Rodriguez-Macia, P.; Dutta, A.; Lubitz, W.; Shaw, W. J.; Ruediger, O. *Angew. Chem., Int. Ed.* **2015**, *54*, 12303−12307.
(16) Reda, T.; Plugge, C. M.; Abram, N. J.; Hirst, J. *Proc. Natl. Acad. Sci. U. S. A.* **2008**, *105*, 10654−10658.
(17) Appel, A.; Bercaw, J.; Bocarsly, A.; Dobbek, H.; DuBois, D.; Dupuis, M.; Ferry, J.; Fujita, E.; Hille, R.; Kenis, P.; Kerfeld, C.; Morris,

DOI: 10.1021/acscatal.7b02736
ACS Catal. 2017, 7, 7558−7566

R.; Peden, C.; Portis, A.; Ragsdale, S.; Rauchfuss, T.; Reek, J.; Seefeldt, L.; Thauer, R.; Waldrop, G. *Chem. Rev.* **2013**, *113*, 6621−6658.
(18) Okura, I. *Biochimie* **1986**, *68*, 189−199.
(19) Bachmeier, A.; Armstrong, F. *Curr. Opin. Chem. Biol.* **2015**, *25*, 141−151.
(20) Woolerton, T. W.; Sheard, S.; Chaudhary, Y. S.; Armstrong, F. A. *Energy Environ. Sci.* **2012**, *5*, 7470−7490.
(21) Lam, Q.; Kato, M.; Cheruzel, L. *Biochim. Biophys. Acta, Bioenerg.* **2016**, *1857*, 589−597.
(22) Reisner, E. *Eur. J. Inorg. Chem.* **2011**, *2011*, 1005−1016.
(23) Brown, K.; Harris, D.; Wilker, M.; Rasmussen, A.; Khadka, N.; Hamby, H.; Keable, S.; Dukovic, G.; Peters, J.; Seefeldt, L.; King, P. *Science* **2016**, *352*, 448−450.
(24) Alonso-Lomillo, M.; Rudiger, O.; Maroto-Valiente, A.; Velez, M.; Rodriguez-Ramos, I.; Munoz, F.; Fernandez, V.; De Lacey, A. *Nano Lett.* **2007**, *7*, 1603−1608.
(25) Rudiger, O.; Gutierrez-Sanchez, C.; Olea, D.; Pereira, I.; Velez, M.; Fernandez, V.; De Lacey, A. *Electroanalysis* **2010**, *22*, 776−783.
(26) Sakimoto, K.; Wong, A.; Yang, P. *Science* **2016**, *351*, 74−77.
(27) Kornienko, N.; Sakimoto, K.; Herlihy, D.; Nguyen, S.; Alivisatos, A.; Harris, C.; Schwartzberg, A.; Yang, P. *Proc. Natl. Acad. Sci. U. S. A.* **2016**, *113*, 11750−11755.
(28) Park, J. H.; Lee, S. H.; Cha, G. S.; Choi, D. S.; Nam, D. H.; Lee, J. H.; Lee, J.-K.; Yun, C.-H.; Jeong, K. J.; Park, C. B. *Angew. Chem., Int. Ed.* **2015**, *54*, 969−973.
(29) Michaelis, L.; Hill, E. S. *J. Gen. Physiol.* **1933**, *16*, 859−873.
(30) Breuer, M.; Rosso, K.; Blumberger, J.; Butt, J. *J. R. Soc., Interface* **2015**, *12*, 20141117.
(31) Nealson, K. H.; Rowe, A. R. *Microb. Biotechnol.* **2016**, *9*, 595−600.
(32) Strycharz-Glaven, S. M.; Snider, R. M.; Guiseppi-Elie, A.; Tender, L. M. *Energy Environ. Sci.* **2011**, *4*, 4366−4379.
(33) Peck, H.; Gest, H. *J. Bacteriol.* **1956**, *71*, 70−80.
(34) Parkinson, B.; Weaver, P. *Nature* **1984**, *309*, 148−149.
(35) Okura, I.; Kimthuan, N. *J. Chem. Soc., Faraday Trans. 1* **1981**, *77*, 1411−1415.
(36) Kreuzer, H. W.; Hill, E. A.; Moran, J. J.; Bartholomew, R. A.; Yang, H.; Hegg, E. L. *FEMS Microbiol. Lett.* **2014**, *352*, 18−24.
(37) Meshulam-Simon, G.; Behrens, S.; Choo, A.; Spormann, A. *Appl. Environ. Microbiol.* **2007**, *73*, 1153−1165.
(38) Shi, L.; Belchik, S.; Plymale, A.; Heald, S.; Dohnalkova, A.; Sybirna, K.; Bottin, H.; Squier, T.; Zachara, J.; Fredrickson, J. *Appl. Environ. Microbiol.* **2011**, *77*, 5584−5590.
(39) Pinchuk, G.; Geydebrekht, O.; Hill, E.; Reed, J.; Konopka, A.; Beliaev, A.; Fredrickson, J. *Appl. Environ. Microbiol.* **2011**, *77*, 8234−8240.
(40) Pinchuk, G. E.; Rodionov, D. A.; Yang, C.; Li, X. Q.; Osterman, A. L.; Dervyn, E.; Geydebrekht, O. V.; Reed, S. B.; Romine, M. F.; Collart, F. R.; Scott, J. H.; Fredrickson, J. K.; Beliaev, A. S. *Proc. Natl. Acad. Sci. U. S. A.* **2009**, *106*, 2874−2879.
(41) Myers, C.; Myers, J. *FEMS Microbiol. Lett.* **1992**, *98*, 13−19.
(42) Kane, A.; Brutinel, E.; Joo, H.; Maysonet, R.; VanDrisse, C.; Kotloski, N.; Gralnick, J. *J. Bacteriol.* **2016**, *198*, 1337−1346.
(43) Bassegoda, A.; Madden, C.; Wakerley, D. W.; Reisner, E.; Hirst, J. *J. Am. Chem. Soc.* **2014**, *136*, 15473−15476.
(44) Maia, L.; Fonseca, L.; Moura, I.; Moura, J. *J. Am. Chem. Soc.* **2016**, *138*, 8834−8846.
(45) Marshall, M.; Plymale, A.; Kennedy, D.; Shi, L.; Wang, Z.; Reed, S.; Dohnalkova, A.; Simonson, C.; Liu, C.; Saffarini, D.; Romine, M.; Zachara, J.; Beliaev, A.; Fredrickson, J. *Environ. Microbiol.* **2007**, *10*, 125−136.
(46) Shukla, A. K.; Suresh, P.; Berchmans, S.; Rajendran, A. *Curr. Sci.* **2004**, *87*, 455−468.
(47) Rabaey, K.; Verstraete, W. *Trends Biotechnol.* **2005**, *23*, 291−298.
(48) Kalyanasundaram, K.; Dung, D. *J. Phys. Chem.* **1980**, *84*, 2551−2556.
(49) Islam, S. D. M.; Konishi, T.; Fujitsuka, M.; Ito, O.; Nakamura, Y.; Usui, Y. *Photochem. Photobiol.* **2000**, *71*, 675−680.
(50) Gurunathan, K.; Maruthamuthu, P.; Sastri, M. V. C. *Int. J. Hydrogen Energy* **1997**, *22*, 57−62.
(51) Crutchley, R. J.; Lever, A. B. P. *J. Am. Chem. Soc.* **1980**, *102*, 7128−7129.
(52) Maruthamuthu, P.; Muthu, S.; Gurunathan, K.; Ashokkumar, M.; Sastri, M. *Int. J. Hydrogen Energy* **1992**, *17*, 863−866.
(53) Honda, Y.; Hagiwara, H.; Ida, S.; Ishihara, T. *Angew. Chem., Int. Ed.* **2016**, *55*, 8045−8048.
(54) Honda, Y.; Watanabe, M.; Hagiwara, H.; Ida, S.; Ishihara, T. *Appl. Catal., B* **2017**, *210*, 400−406.
(55) Krasnovsky, A.; Nikandrov, V. *FEBS Lett.* **1987**, *219*, 93−96.
(56) Gross, M. A.; Reynal, A.; Durrant, J. R.; Reisner, E. *J. Am. Chem. Soc.* **2014**, *136*, 356−366.
(57) Gillaizeau-Gauthier, I.; Odobel, F.; Alebbi, M.; Argazzi, R.; Costa, E.; Bignozzi, C. A.; Qu, P.; Meyer, G. J. *Inorg. Chem.* **2001**, *40*, 6073−6079.
(58) Kirch, M.; Lehn, J.; Sauvage, J. *Helv. Chim. Acta* **1979**, *62*, 1345−1384.
(59) Pellegrin, Y.; Odobel, F. *C. R. Chim.* **2017**, *20*, 283−295.
(60) Vincent, K.; Parkin, A.; Armstrong, F. *Chem. Rev.* **2007**, *107*, 4366−4413.
(61) Batistela, V.; Pellosi, D.; de Souza, F.; da Costa, W.; Santin, S.; de Souza, V.; Caetano, W.; de Oliveira, H.; Scarminio, I.; Hioka, N. *Spectrochim. Acta, Part A* **2011**, *79*, 889−897.
(62) Sakai, T.; Mersch, D.; Reisner, E. *Angew. Chem., Int. Ed.* **2013**, *52*, 12313−12316.
(63) Jones, R. W.; Garland, P. B. *Biochem. J.* **1977**, *164*, 199−211.
(64) Liu, J.; Wang, Z.; Belchik, S.; Edwards, M.; Liu, C.; Kennedy, D.; Merkley, E.; Lipton, M.; Butt, J.; Richardson, D.; Zachara, J.; Fredrickson, J.; Rosso, K.; Shi, L. *Front. Microbiol.* **2012**, DOI: 10.3389/fmicb.2012.00037.
(65) Dai, J.; Wei, H.; Tian, C.; Damron, F.; Zhou, J.; Qiu, D. *BMC Microbiol.* **2015**, *15*, 34.
(66) Caputo, C.; Wang, L.; Beranek, R.; Reisner, E. *Chem. Sci.* **2015**, *6*, 5690−5694.
(67) McLaughlin, M.; McCormick, T.; Eisenberg, R.; Holland, P. *Chem. Commun.* **2011**, *47*, 7989−7991.
(68) Van Beeumen, J.; Leys, D.; Tsapin, A.; Nealson, K.; Meyer, T.; Cusanovich, M. *Nat. Struct. Biol.* **1999**, *6*, 1113−1117.
(69) Martindale, B.; Joliat, E.; Bachmann, C.; Alberto, R.; Reisner, E. *Angew. Chem., Int. Ed.* **2016**, *55*, 9402−9406.
(70) Kirchhofer, N. D.; Rengert, Z. D.; Dahlquist, F. W.; Nguyen, T.-Q.; Bazan, G. C. *Chem.* **2017**, *2*, 240−257.
(71) Ainsworth, E.; Lockwood, C.; White, G.; Hwang, E.; Sakai, T.; Gross, M.; Richardson, D.; Clarke, T.; Jeuken, L.; Reisner, E.; Butt, J. *ChemBioChem* **2016**, *17*, 2324−2333.

DOI: 10.1021/acscatal.7b02736
ACS Catal. 2017, 7, 7558−7566